

Class Label-aware Graph Anomaly Detection

Junghoon Kim
KAIST GSDS
Daejeon, Republic of Korea
jkhkim611@kaist.ac.kr

Yeonjun In
KAIST ISysE
Daejeon, Republic of Korea
yeonjun.in@kaist.ac.kr

Kanghoon Yoon
KAIST ISysE
Daejeon, Republic of Korea
ykhoo08@kaist.ac.kr

Junmo Lee
KAIST ISysE
Daejeon, Republic of Korea
bubblego0217@kaist.ac.kr

Chanyoung Park*
KAIST ISysE & AI
Daejeon, Republic of Korea
cy.park@kaist.ac.kr

ABSTRACT

Unsupervised GAD methods assume the lack of anomaly labels, i.e., whether a node is anomalous or not. One common observation we made from previous unsupervised methods is that they not only assume the absence of such anomaly labels, but also the *absence of class labels* (the class a node belongs to used in a general node classification task). In this work, we study the utility of class labels for unsupervised GAD; in particular, how they enhance the detection of *structural anomalies*. To this end, we propose a Class Label-aware Graph Anomaly Detection framework (CLAD) that utilizes a limited amount of labeled nodes to enhance the performance of unsupervised GAD. Extensive experiments on ten datasets demonstrate the superior performance of CLAD in comparison to existing unsupervised GAD methods, even in the absence of ground-truth class label information. The source code for CLAD is available at <https://github.com/jkhkim611/CLAD>.

CCS CONCEPTS

• Computing methodologies → Artificial intelligence.

KEYWORDS

Anomaly Detection, Attributed Graphs, Graph Neural Networks

ACM Reference Format:

Junghoon Kim, Yeonjun In, Kanghoon Yoon, Junmo Lee, and Chanyoung Park. 2023. Class Label-aware Graph Anomaly Detection. In *Proceedings of the 32nd ACM International Conference on Information and Knowledge Management (CIKM '23)*, October 21–25, 2023, Birmingham, United Kingdom. ACM, New York, NY, USA, 5 pages. <https://doi.org/10.1145/3583780.3615249>

1 INTRODUCTION

Anomalies in real-world graphs can manifest as frauds in telecommunications networks [1, 21], fake reviews in user rating systems [17], or illicit transactions in financial networks [20]. Many

*Corresponding author

Permission to make digital or hard copies of all or part of this work for personal or classroom use is granted without fee provided that copies are not made or distributed for profit or commercial advantage and that copies bear this notice and the full citation on the first page. Copyrights for components of this work owned by others than the author(s) must be honored. Abstracting with credit is permitted. To copy otherwise, or republish, to post on servers or to redistribute to lists, requires prior specific permission and/or a fee. Request permissions from permissions@acm.org.
CIKM '23, October 21–25, 2023, Birmingham, United Kingdom
© 2023 Copyright held by the owner/author(s). Publication rights licensed to ACM.
ACM ISBN 979-8-4007-0124-5/23/10...\$15.00
<https://doi.org/10.1145/3583780.3615249>

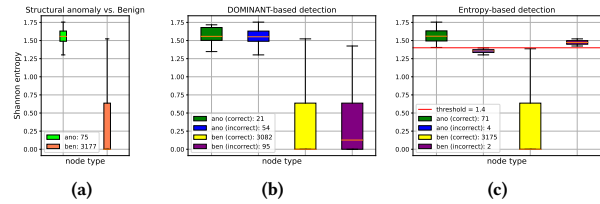


Figure 1: (a) Average Shannon entropy of the neighborhood class distribution of structural anomalies/benign nodes. (b) GAD result of DOMINANT [3]. (c) GAD result of an entropy-based method, where the red horizontal line indicates the threshold (In (b) and (c), green/blue boxes indicate correctly/incorrectly classified structural anomalies, and yellow/purple boxes indicate correctly/incorrectly classified benign nodes. The number of nodes in each group is shown).

Graph Anomaly Detection (GAD) studies employ Graph Neural Networks (GNNs) due to their superior performance on various downstream tasks [8, 9, 19, 22]. A line of research for GAD adopts a supervised learning setting - where nodes are labeled as anomalous or benign - and solves a binary classification problem to detect anomalies [2, 4, 12, 13]. However, obtaining ground-truth anomaly labels is not an easy task. For many real-world cases, only a small fraction of anomalous samples are annotated as such [11], which makes the utilization of supervised methods in such scenarios comparatively cumbersome.

On the other hand, unsupervised GAD methods assume the absence of such labels, which is a more realistic scenario. Previous studies [3, 14] categorize a node's malicious behaviors into *structural anomalies* - nodes that exhibit abnormal connections with other nodes - and *attribute anomalies* - nodes whose attributes significantly differ from those of their neighbors. Recent works [3, 15] have employed GNN-based autoencoders to assign anomaly scores to individual nodes based on reconstruction errors. Specifically, one GNN is trained to capture the structural information of nodes, while the other is trained to capture attribute information. The anomaly score for each node is computed as a weighted sum of the reconstruction errors from both GNNs, which do not require any anomaly label information.

One common observation we made from previous unsupervised methods is that they not only assume the absence of anomaly labels (whether node is anomalous used in an anomaly detection task), but also the *absence of class labels* (the class a node belongs to used in a general node classification task). However, since a structural

anomaly tends to exhibit abnormal behaviors in its vicinity (i.e., neighbors) in terms of class distribution, we find that the class label information of nodes is indeed beneficial for the GAD task. In Fig. 1a, we show the average Shannon entropy of the neighborhood class distribution for both structural anomalies and benign nodes in Citeseer dataset. We clearly observe that the vast majority of benign nodes have a lower entropy compared with that of structural anomalies, indicating that structural anomalies tend to have neighboring nodes with a higher variety of classes. Based on this observation, in Fig. 1c, we used the entropy value as a threshold (red line) to distinguish between structural anomalies and benign nodes. Surprisingly, we greatly outperformed the anomaly detection performance of an existing unsupervised GAD method, DOMINANT [3], shown in Fig. 1b, i.e., we reduced the number of anomalies that are incorrectly classified as benign (54→4), and decreased the number of benign nodes that are incorrectly classified as anomalous (95→2) as well.

Inspired by our observations in Fig. 1, we focus on the utility of class labels for unsupervised GAD. More specifically, we study how the class label information of nodes enhances the detection of *structural anomalies* in particular. In fact, the experiments in Fig. 1 are conducted assuming that the node labels are known for all nodes, which explains the superior performance of a simple entropy-based anomaly detection approach as shown in Fig. 1c. However, since only a small fraction of nodes in real-world graphs are typically labeled, it becomes crucial to effectively utilize the limited amount of labeled nodes available.

To this end, we propose a Class Label-aware Graph Anomaly Detection framework (CLAD) that utilizes a limited amount of labeled nodes to enhance the performance of unsupervised GAD. More precisely, the main component of CLAD is the structural anomaly quantifier that uses the output of a GNN-based node classifier to compute the discrepancy (i.e., Jensen-Shannon Divergence (JSD)) between the *predicted* class distribution of a node and the average of its neighboring nodes.

However, we discovered that the JSD value computed between a node and its neighboring nodes is highly dependent on the degree of the node. In other words, introducing an additional neighbor to a low-degree node would significantly impact the JSD value, whereas adding such a neighbor to a high-degree node would result in a negligible change. Hence, we propose a modified JSD, i.e., JSD+, to take into account the node degree information. Moreover, attribute anomalies are identified through an attribute anomaly quantifier, which is designed to compute the discrepancy between the attributes of a node and its neighboring nodes. In the end, we combine the anomaly scores obtained from the structural/attribute anomaly quantifiers to obtain the final anomaly score of each node.

Through extensive experiments, we demonstrate that CLAD outperforms existing unsupervised GAD methods, even when the ratio of known labels is extremely small. Moreover, even in an extreme case where no class labels are available at all, pseudo-labels constructed from simple attribute-based clustering techniques are enough for CLAD to successfully distinguish anomalies from benign nodes. This shows that the framework is suitable for application even in scenarios where obtaining class labels is difficult. To the best of our knowledge, this is the first work to consider class labels of nodes for unsupervised GAD.

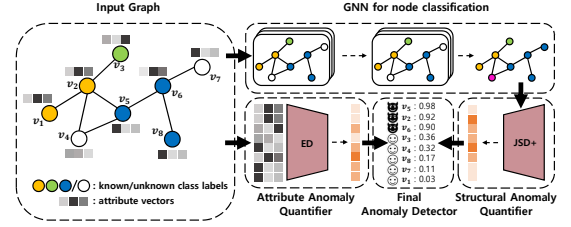


Figure 2: Overall framework of CLAD

2 PROBLEM STATEMENT

Definition. Let $\mathcal{G} = (\mathcal{V}, \mathcal{E}, \mathcal{A}, \mathcal{X})$ denote an undirected attributed graph, where \mathcal{V} is the set of N nodes, \mathcal{E} is the set of edges between these nodes and $\mathcal{X} \in \mathbb{R}^{N \times F}$ contains the node attributes. $\mathcal{A} \in \mathbb{R}^{N \times N}$ is the adjacency matrix, in which $\mathcal{A}_{ij} = 1$ indicates v_i and v_j are linked and $\mathcal{A}_{ij} = 0$ otherwise. F is the number of node attributes and $x_i = \mathcal{X}[i, :] \in \mathbb{R}^F$ indicates the attribute vector of node v_i .

Problem. Given an attributed graph $\mathcal{G} = (\mathcal{V}, \mathcal{E}, \mathcal{A}, \mathcal{X})$, our goal is to detect the nodes whose characteristics significantly deviate from the majority of other nodes in terms of structure and attributes. More specifically, we aim to give a numeric score $y_i \in [0, 1]$ for each node v_i such that a node with high y_i is deemed anomalous. Note that as an unsupervised method we do not have access to nodes' anomaly labels, but we do have information on a portion of nodes' class labels, where C denotes the number of classes.

3 METHOD

Fig. 2 illustrates the overall architecture of CLAD. First, a GNN for node classification is trained in a semi-supervised manner using the known class labels. Here, ground-truth class labels are used when available; when not, pseudo-labels obtained from simple clustering algorithms on the node attributes can be used. We then devise *two modules to measure the structural and attribute anomaly* of a node. The final anomaly score for each node is calculated as a *weighted sum of the scores* from both modules.

3.1 Structural Anomaly Quantifier

Jensen-Shannon Divergence (JSD) [10] is a metric that measures the divergence of a set of probabilities, which is defined as:

$$JSD(i) = H\left(\frac{1}{|\mathcal{N}(i)|} \sum_{j \in \mathcal{N}(i)} p_j\right) - \frac{1}{|\mathcal{N}(i)|} \sum_{j \in \mathcal{N}(i)} H(p_j) \quad (1)$$

where $p_j \in \mathbb{R}^C$ is the output softmax probabilities of a GNN for node v_j . Regarding p_j as a probability mass function over possible class labels, $H(p_j) = -\sum_c p_{jc} \cdot \log(p_{jc})$ is the Shannon entropy of p_j , where p_{jc} is the probability of node v_j belonging to class $c \in [1, 2, \dots, C]$. $\mathcal{N}(i)$ is the set of 1-hop neighboring nodes of a node v_i including the node itself, i.e., v_i . In short, $JSD(i)$ is increased when the discrepancy in the class distribution of node v_i and its neighboring nodes $\mathcal{N}(i)$ becomes greater. From Fig. 1, we can expect the JSD values of structural anomalies to be higher than those of benign nodes. Moreover, the first plot of Fig. 3c shows a fairly clear distinction in the $\log(JSD)$ value between structural anomalies (in green) and benign nodes (in red), indicating that JSD can indeed be used as a metric for detecting structural anomalies.

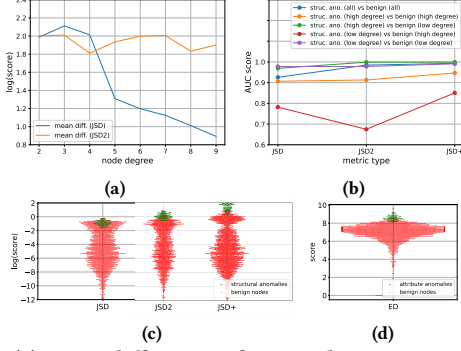


Figure 3: (a) Mean difference of JSD and JSD2 scores between structural anomalies and benign nodes over node degrees. (b) ROC-AUC scores for JSD, JSD2 and JSD+ distinguishing nodes of different node degree groups. (c) Swarm plots of JSD, JSD2 and JSD+ scores for structural anomalies and benign nodes. (d) Swarm plot of ED scores for attribute anomalies and benign nodes. Citeseer dataset is used.

Addressing node degree-bias issue in JSD. However, naively utilizing JSD in its base form has one major drawback. That is, when neighboring nodes are added/deleted, the JSD value of a relatively low-degree structural anomaly would be largely affected, while a high-degree structural anomaly would see a negligible change. This would make it difficult to differentiate high-degree structural anomalies and benign nodes, potentially hindering the effectiveness of JSD. To alleviate this node degree-bias issue, we consider the node degree in a way that maintains an appropriate difference in the values, which can be achieved by simply multiplying the node degree with the JSD value: $JSD2(i) = JSD(i) \cdot \log(\text{degree}_i)$. In Fig. 3a we can see our intuition in action - for JSD the difference between structural anomalies and benign nodes sharply declines with an increase in the node degree, while for JSD2 anomalies maintain this difference. Moreover, Fig. 3c shows that JSD2 better distinguishes structural anomalies from benign nodes.

Yet, while JSD2 alleviates the problem of *difference between scores*, it runs into a new issue regarding the *actual value of scores*. Specifically, by multiplying the node degree with the JSD value, we are at risk of obtaining an extremely large value for high-degree nodes regardless of their anomaly, which is not desired. Consequently, JSD2 can potentially predict benign nodes to be anomalous if their node degree is high, and vice versa for low-degree structural anomalies. This is evident in Fig. 3b, where we observe that JSD2 struggles more in distinguishing low-degree structural anomalies from high-degree benign nodes (as depicted by the red line).

This issue can be handled by using a value that doesn't become too large for high-degree benign nodes. Based on our observation in Fig. 1, we can expect that a benign node's neighboring nodes are likely to share the same class label as the benign node itself, while the opposite holds for structural anomalies. Thus, defining the number of neighboring nodes whose predicted class is the same as node v_i as $\gamma_i = \sum_{j \in \mathcal{N}(i)} (\arg \max_c p_i == \arg \max_c p_j)$ (note that for obtaining γ_i , $v_i \notin \mathcal{N}(i)$), the value $(\text{degree}_i - \gamma_i)$ will tend to be small for benign nodes and large for structural anomalies. Utilizing this value we devise a new metric: $JSD+(i) = JSD(i) \cdot \log(\text{degree}_i - \gamma_i)$. JSD+ addresses the aforementioned problem by giving less weight to the node degree of benign nodes. In Figs. 3b and 3c, we observe

Table 1: Statistics of the datasets used for experiments

Dataset	N	$ \mathcal{E} $	F	# Anomalies	# Labeled nodes	Class labels given?
Cora	2708	5803	1433	150	812 (30%)	
Citeseer	3327	5077	3703	150	998 (30%)	
Amazon Computers	13752	245861	767	750	4125 (30%)	○
Amazon Photo	7650	119081	745	450	2295 (30%)	
ogbn-arxiv	169343	1249671	128	7500	50802 (30%)	
Automotive	28922	106650	300	3173		
Patio, Lawn and Garden	30982	124740	300	3173	-	×
Office Products	47138	487848	300	3226		
Yelp	45954	3846979	32	6677	-	×
Elliptic	46564	73248	93	4545		

that JSD+ improves significantly over JSD and JSD2, especially in discriminating low-degree structural anomalies from high-degree benign nodes. Thus, our *structural anomaly quantifier* uses JSD+ to represent the structural anomaly of each node.

3.2 Attribute Anomaly Quantifier

To detect attribute anomalies, we compute the discrepancy of a node's attributes compared to its neighboring nodes' attributes. We first define the divergence between two nodes v_i and v_j as $\text{dist}(i, j) = \|x_i - x_j\|_2$ i.e., the Euclidean distance. Then, the discrepancy metric used for our *attribute anomaly quantifier* is defined as: $ED(i) = \frac{1}{|\mathcal{N}(i)|} \sum_{j \in \mathcal{N}(i)} \text{dist}(i, j)$, where $\mathcal{N}(i)$ is the set of 1-hop neighboring nodes of a node v_i , and we take the mean over the distances so that the number of neighbors does not affect the score. We expect the ED values to be high for attribute anomalies as their attributes would significantly differ from those of their neighbors. In Fig. 3d, we observe that the ED values clearly distinguish attribute anomalies from benign nodes.

Final Anomaly Detector. We compute the final anomaly score for node v_i as a weighted sum of its structural and attribute anomaly scores [3, 5, 15]: $y_i = \alpha \cdot \text{struc}_i + (1 - \alpha) \cdot \text{attr}_i$, where struc_i and attr_i are the JSD+ and ED values obtained from the previous two modules scaled to be in range [0, 1], respectively, and $\alpha \in [0, 1]$ is a hyperparameter that balances the two scores. After ranking the final anomaly score for each node in descending order, we consider the nodes with high rank as anomalous.

4 EXPERIMENTS

Datasets. We conduct extensive experiments on ten widely used datasets, which can be divided into three categories. (1) **Synthetic1:** We use five benchmark datasets [6, 16, 18] in which anomalies are added following a previous well-known anomaly injection scheme [3] (i.e., Cora, Citeseer, Amazon Computers, Amazon Photo, and ogbn-arxiv). (2) **Synthetic2:** We create three datasets in which nodes are users in Amazon, edges denote the co-review relationship between the users, and node attributes are the pre-trained embeddings of the reviews written by each user. We assume that an anomalous user writes fake reviews to random items, and this leads to anomalous links in our generated datasets (i.e., Automotive, Patio, Lawn and Garden, and Office Products). *Synthetic2* datasets' anomalies follow a more realistic scenario than that of *Synthetic1* datasets. (3) **Real-world:** We use two datasets [17, 20] that contain real-world anomalies (i.e., Yelp and Elliptic). Data statistics are summarized in Table 1. Note that ground-truth class labels are only present for *Synthetic1* datasets.

Baselines. We compare CLAD with the following methods: DOMINANT [3], CoLA [14], ANEMONE [7], AnomalyDAE [5] and ComGA [15]. We additionally include variants of DOMINANT and COLA, i.e., DOMINANT2 and CoLA2, by adding a cross-entropy

Table 2: AUC score (%) of CLAD and baselines on all datasets. The computation time(s) is included in parantheses.

	Cora	Citeseer	Amz. Com.	Amz. Pho.	ogbn-arxiv	Automotive	PL&G	Office Products	Yelp	Elliptic
DOMINANT	89.6 (9.5)	87.4 (24.4)	63.4 (106.4)	64.3 (35.1)	77.9 (6651.7)	72.4 (350.9)	82.7 (407.2)	33.6 (904.5)	48.9 (740.4)	16.0 (790.2)
CoLA	89.9 (628.3)	89.7 (667.5)	68.5 (2513.3)	69.1 (1402.9)	80.3 (28704.6)	85.5 (4268.8)	86.0 (5131.4)	81.3 (7158.4)	43.6 (9314.6)	18.5 (6259.1)
ANEMONE	91.0 (256.4)	91.9 (542.2)	65.1 (2321.8)	65.9 (1184.7)	80.2 (24026.5)	60.9 4919.3)	66.9 (5094.6)	67.0 (7968.0)	41.8 (9503.1)	23.4 (6018.7)
AnomalyDAE	84.5 (10.1)	82.6 (27.2)	67.1 (116.8)	67.6 (33.2)	72.1 (7023.9)	77.5 (344.6)	74.1 (421.1)	76.4 (1046.5)	36.1 (767.0)	14.7 (819.6)
ComGA	92.2 (11.2)	90.9 (26.7)	69.7 (127.6)	70.1 (36.7)	81.0 (7203.5)	73.4 (367.0)	77.1 (448.6)	82.5 (943.8)	49.5 (786.3)	17.1 (847.9)
DOMINANT2	89.1 (17.4)	85.4 (17.6)	63.1 (32.7)	63.9 (20.9)	77.5 (1543.8)	71.1 (55.8)	78.6 (59.9)	34.7 (146.7)	49.2 (190.3)	15.9 (175.8)
CoLA2	76.9 (467.2)	76.8 (933.7)	60.6 (3511.2)	59.8 (2238.0)	75.3 (40171.4)	75.3 (6515.2)	66.2 (6528.6)	66.4 (10432.3)	39.7 (12148.8)	18.7 (8041.0)
CLAD (ours)	94.9 (3.5)	97.3 (3.7)	75.6 (28.1)	79.0 (14.8)	84.6 (1322.1)	91.6 (47.2)	89.8 (53.6)	88.1 (139.5)	56.3 (173.6)	49.4 (50.2)

Table 3: AUC score (%) of CLAD and baselines on three datasets. We report the results for detecting structural (s.) and attribute (a.) anomalies separately.

	DOMINANT		CoLA		ANEMONE		AnomalyDAE		ComGA		DOMINANT2		CoLA2		CLAD (ours)	
	s.	a.	s.	a.	s.	a.	s.	a.	s.	a.	s.	a.	s.	a.	s.	a.
Citeseer	77.0	95.8	93.2	80.9	96.4	87.5	88.2	81.5	94.3	82.6	73.9	95.2	87.2	65.2	99.3	97.7
Amz. Com.	69.8	55.9	79.2	54.6	73.0	50.2	78.8	52.0	80.3	51.5	69.9	55.6	68.1	50.2	93.1	64.9
Amz. Pho.	69.4	58.3	78.1	57.9	72.5	54.4	76.9	58.1	79.4	56.0	69.0	58.0	65.3	51.7	96.5	68.7

Table 4: AUC score (%) of CLAD on three datasets while reducing the ratio/number of known class labels.

	30%	10%	5%	1%	10	1
Citeseer	97.3	96.6	96.4	94.1	90.2	86.4
Amz. Com.	75.6	74.9	74.9	74.6	71.9	58.8
Amz. Pho.	79.0	78.9	78.8	78.8	70.7	57.3

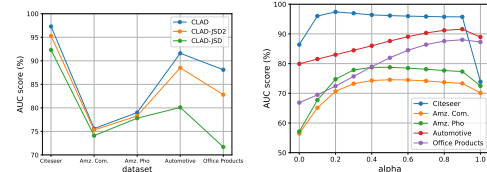
loss for the node classification task to their respective objective functions. For all baselines, we use the official codes published by the authors, including the hyperparameter settings.

Implementation Details. We use a two-layer GCN [9] as the backbone GNN. For *Synthetic1* datasets, we randomly sample 30% of the ground-truth class labels. For *Synthetic2* and *Real-world* datasets that do not contain ground-truth class label information, we assign a pseudo-label to each node via K-means clustering with 5 clusters based on the node attributes. We then disregard all class label information except for the 50 nodes closest to each cluster centroid, i.e., we only have knowledge on 250 class labels, 50 per class. For all datasets the backbone GNN classifier is trained on 95% of these *known class labels* and validated on the remaining 5%. We find the best performing α from [0.0, 0.1, 0.2, ..., 0.9, 1.0]. The average value of five independent runs is reported for all results. We adopt the ROC-AUC metric to evaluate the performance of anomaly detection.

4.1 Performance Analysis

General Performance. Table 2 shows that CLAD outperforms all baselines on *Synthetic1* datasets, proving the effectiveness of our method in detecting anomalies present in graph data. This is further supported by Table 3, which reports the detection performance in terms of structural and attribute anomalies separately. These results demonstrate the effectiveness of our proposed metrics. By comparing with DOMINANT2 and CoLA2, we can observe that naively using the class label information falls short of improving the detection performance, further proving the soundness of our proposed method. As a further appeal, we emphasize that CLAD achieves superior performance even while consuming much less computational time (GCN training and calculating scores) than baselines, which is especially beneficial for massive datasets like ogbn-arxiv. This shows the practicality of CLAD in the real-world.

Reducing the ratio/number of known class labels. We further report the performance of CLAD for cases in which only a few nodes are labeled with class information. Table 4 shows that reducing

**Figure 4: (a) AUC scores (%) for CLAD and its two variants. (b) Effect of parameter α on CLAD's detection performance.**

the ratio down to 1% only incrementally hinders the performance. Even with access to only a handful (e.g., 10) of class labels, CLAD produces results comparable to that of baselines.

Lack of class labels. As previously mentioned, experiments on *Synthetic2* and *Real-world* datasets are conducted under the assumption that *class labels are not available*. In Table 2, we observe that CLAD still outperforms all baselines even with pseudo-labels obtained based on node attributes. Note that CLAD shows significant performance gain especially in *Real-world* datasets. We argue that these results demonstrate the practicality of CLAD in real-world scenarios where the class label information may be missing.

Ablation Study. We compare the results of CLAD with two variants that replace *JSD+* with *JSD* and *JSD2*, respectively. Fig. 4a shows that the original CLAD model outperforms both CLAD-JSD2 and CLAD-JSD. Since the output of the attribute anomaly quantifier does not change, the performance differences only stem from the choice of the metric in the *structural anomaly quantifier*. This demonstrates the superiority of *JSD+* over *JSD* and *JSD2*.

Hyperparameter Sensitivity. We investigate the sensitivity of parameter α . In Fig. 4b, we observe that α should be set to a value between 0 and 1, indicating that jointly taking into account both perspectives of anomalies is important for achieving high detection performance. Moreover, an optimal α differs across datasets.

5 CONCLUSION

In this paper, we propose a Class Label-aware Graph Anomaly Detection framework (CLAD) that utilizes a limited amount of labeled nodes to enhance the performance of unsupervised GAD. Specifically, based on our empirical analysis that the vast majority of benign nodes have a much lower entropy of the neighborhood class distribution compared with that of structural anomalies, we devise a metric, called *JSD+*, that effectively and efficiently distinguishes structural anomalies from benign nodes. Extensive experimental results demonstrate that CLAD outperforms existing unsupervised GAD methods, even in the absence of ground-truth class label information - indicating CLAD's versatility in real-world scenarios.

Acknowledgement. No.2022-0-00077 and No.2021R1C1C1009081.

REFERENCES

- [1] Leman Akoglu, Hanghang Tong, and Danai Koutra. 2015. Graph based anomaly detection and description: a survey. *Data mining and knowledge discovery* 29 (2015), 626–688.
- [2] Ziwei Chai, Siqi You, Yang Yang, Shiliang Pu, Jiarong Xu, Haoyang Cai, and Weihao Jiang. 2022. Can Abnormality be Detected by Graph Neural Networks?. In *Proceedings of the Twenty-Ninth International Joint Conference on Artificial Intelligence (IJCAI)*, Vienna, Austria. 23–29.
- [3] Kaize Ding, Jundong Li, Rohit Bhanushali, and Huan Liu. 2019. Deep anomaly detection on attributed networks. In *Proceedings of the 2019 SIAM International Conference on Data Mining*. SIAM, 594–602.
- [4] Yingdong Dou, Zhiwei Liu, Li Sun, Yutong Deng, Hao Peng, and Philip S Yu. 2020. Enhancing graph neural network-based fraud detectors against camouflaged fraudsters. In *Proceedings of the 29th ACM International Conference on Information & Knowledge Management*. 315–324.
- [5] Haoyi Fan, Fengbin Zhang, and Zuoyong Li. 2020. Anomalydae: Dual autoencoder for anomaly detection on attributed networks. In *ICASSP 2020-2020 IEEE International Conference on Acoustics, Speech and Signal Processing (ICASSP)*. IEEE, 5685–5689.
- [6] Weihua Hu, Matthias Fey, Marinka Zitnik, Yuxiao Dong, Hongyu Ren, Bowen Liu, Michele Catasta, and Jure Leskovec. 2020. Open graph benchmark: Datasets for machine learning on graphs. *Advances in neural information processing systems* 33 (2020), 22118–22133.
- [7] Ming Jin, Yixin Liu, Yu Zheng, Lianhua Chi, Yuan-Fang Li, and Shirui Pan. 2021. Anemone: Graph anomaly detection with multi-scale contrastive learning. In *Proceedings of the 30th ACM International Conference on Information & Knowledge Management*. 3122–3126.
- [8] Wei Jin, Yao Ma, Xiaorui Liu, Xianfeng Tang, Suhang Wang, and Jiliang Tang. 2020. Graph structure learning for robust graph neural networks. In *Proceedings of the 26th ACM SIGKDD international conference on knowledge discovery & data mining*. 66–74.
- [9] Thomas N Kipf and Max Welling. 2016. Semi-supervised classification with graph convolutional networks. *arXiv preprint arXiv:1609.02907* (2016).
- [10] Jianhua Lin. 1991. Divergence measures based on the Shannon entropy. *IEEE Transactions on Information theory* 37, 1 (1991), 145–151.
- [11] Fanzhen Liu, Zhao Li, Baokun Wang, Jia Wu, Jian Yang, Jiaming Huang, Yiqing Zhang, Weiqiang Wang, Shan Xue, Surya Nepal, et al. 2022. eRiskCom: an e-commerce risky community detection platform. *The VLDB Journal* 31, 5 (2022), 1085–1101.
- [12] Fanzhen Liu, Xiaoxiao Ma, Jia Wu, Jian Yang, Shan Xue, Amin Beheshti, Chuan Zhou, Hao Peng, Quan Z Sheng, and Charu C Aggarwal. 2022. DAGAD: Data Augmentation for Graph Anomaly Detection. *arXiv preprint arXiv:2210.09766* (2022).
- [13] Yang Liu, Xiang Ao, Zidi Qin, Jianfeng Chi, Jinghua Feng, Hao Yang, and Qing He. 2021. Pick and choose: a GNN-based imbalanced learning approach for fraud detection. In *Proceedings of the Web Conference 2021*. 3168–3177.
- [14] Yixin Liu, Zhao Li, Shirui Pan, Chen Gong, Chuan Zhou, and George Karypis. 2021. Anomaly detection on attributed networks via contrastive self-supervised learning. *IEEE transactions on neural networks and learning systems* 33, 6 (2021), 2378–2392.
- [15] Xuexiong Luo, Jia Wu, Amin Beheshti, Jian Yang, Xiankun Zhang, Yuan Wang, and Shan Xue. 2022. Comga: Community-aware attributed graph anomaly detection. In *Proceedings of the Fifteenth ACM International Conference on Web Search and Data Mining*. 657–665.
- [16] Julian McAuley, Christopher Targett, Qinfeng Shi, and Anton Van Den Hengel. 2015. Image-based recommendations on styles and substitutes. In *Proceedings of the 38th international ACM SIGIR conference on research and development in information retrieval*. 43–52.
- [17] Shebuti Rayana and Leman Akoglu. 2015. Collective opinion spam detection: Bridging review networks and metadata. In *Proceedings of the 21th acm sigkdd international conference on knowledge discovery and data mining*. 985–994.
- [18] Prithviraj Sen, Galileo Namata, Mustafa Bilgic, Lise Getoor, Brian Galligher, and Tina Eliassi-Rad. 2008. Collective classification in network data. *AI magazine* 29, 3 (2008), 93–93.
- [19] Petar Veličković, Guillem Cucurull, Arantxa Casanova, Adriana Romero, Pietro Lio, and Yoshua Bengio. 2017. Graph attention networks. *arXiv preprint arXiv:1710.10903* (2017).
- [20] Mark Weber, Giacomo Domeniconi, Jie Chen, Daniel Karl I Weidele, Claudio Bellei, Tom Robinson, and Charles E Leiserson. 2019. Anti-money laundering in bitcoin: Experimenting with graph convolutional networks for financial forensics. *arXiv preprint arXiv:1908.02591* (2019).
- [21] Yang Yang, Yuhong Xu, Yizhou Sun, Yuxiao Dong, Fei Wu, and Yueting Zhuang. 2019. Mining fraudsters and fraudulent strategies in large-scale mobile social networks. *IEEE Transactions on Knowledge and Data Engineering* 33, 1 (2019), 169–179.
- [22] Dingyuan Zhu, Ziwei Zhang, Peng Cui, and Wenwu Zhu. 2019. Robust graph convolutional networks against adversarial attacks. In *Proceedings of the 25th*